

## Research Paper

# Engineered Zn(II)-Dipicolylamine-Gold Nanorod Provides Effective Prostate Cancer Treatment by Combining siRNA Delivery and Photothermal Therapy

Kyung Hyun Min<sup>1,2</sup>, Young-Hwa Kim<sup>1</sup>, Zhantong Wang<sup>1</sup>, Jihoon Kim<sup>1</sup>, Jee Seon Kim<sup>1</sup>, Sun Hwa Kim<sup>2</sup>, Kwangmeyung Kim<sup>2</sup>, Ick Chan Kwon<sup>2</sup>, Dale O. Kiesewetter<sup>1</sup>, and Xiaoyuan Chen<sup>1</sup>✉

1. Laboratory of Molecular Imaging and Nanomedicine, National Institute of Biomedical Imaging and Bioengineering, National Institutes of Health, Bethesda, Maryland 20892, United States;
2. Center for Theragnosis, Biomedical Research Institute, Korea Institute of Science and Technology, Seoul 136-791, Republic of Korea.

✉ Corresponding author: shawn.chen@nih.gov

© Ivyspring International Publisher. This is an open access article distributed under the terms of the Creative Commons Attribution (CC BY-NC) license (<https://creativecommons.org/licenses/by-nc/4.0/>). See <http://ivyspring.com/terms> for full terms and conditions.

Received: 2017.08.18; Accepted: 2017.08.28; Published: 2017.09.26

## Abstract

Combination cancer treatment has emerged as a critical approach to achieve remarkable anticancer effect. In this study, we prepared a theranostic nanoformulation that allows for photoacoustic imaging as well as combination gene and photothermal therapy. Gold nanorods (GNR) were coated with dipicolyl amine (DPA), which forms stable complexes with Zn<sup>2+</sup> cations. The resulting nanoparticles, Zn(II)/DPA-GNR, recognize phosphate-containing molecules, including siRNA, because of the specific interaction between Zn(II) and the phosphates. We chose anti-polo-like kinase 1 siRNA (siPLK) as our example for gene silencing. The strong complexation between Zn(II)/DPA-GNR and siPLK provided high stability to the nano-complexes, which efficiently delivered siRNA into the targeted cancer cells *in vitro* and *in vivo*. The particle served as a theranostic agent because the GNRs of nano-complexes permitted effective photothermal therapy as well as photoacoustic imaging upon laser irradiation. This gene/photothermal combination therapy using siPLK/Zn(II)DPA-GNRs exhibited significant antitumor activity in a PC-3 tumor mouse model. The concept described in this work may be extended to the development of efficient delivery strategies for other polynucleotides as well as advanced anticancer therapy.

Key words: dipicolylamine, metal-organic complexes, siRNA, gold nanorod, photothermal therapy, photoacoustic imaging, combination therapy, theranostics.

## Introduction

RNA interference (RNAi) has been widely used for cancer therapy because of its naturally occurring unique sequence-specific post-transcriptional gene silencing effect. Recently significant progresses have been made in this research field.(1-3) However, due to the anionic charge of siRNA phosphodiester backbone and its large molecular weight, the delivery of siRNA based therapeutics is restricted by a relatively poor pharmacokinetics and low cellular internalization following systemic administration (4, 5). Despite promising pre-clinical studies, there are

currently no clinically successful siRNA formulations for tumor treatment. Although numerous tumor therapeutic siRNA delivery carriers have been developed based on cationic polymers, cationic lipids, or amino acids that efficiently bind anionic RNAi, such as small interfering RNA (siRNA) and microRNA (miRNA) (6-9), these strong cationic carriers cause destabilization of cell membranes and severe cytotoxicity to normal tissues (10-14). This non-specific cell cytotoxicity has proven to be a major barrier in the clinical application of RNAi delivery

systems. To overcome these limitations, more study is required to develop efficient siRNA delivery nanoplateforms without using strong cationic derivatives.

Recently, we developed a hyaluronic acid (HA)-based nanoparticle system for delivering siRNA that uses Zn(II)-dipicolylamine (Zn-DPA) receptors for high siRNA binding affinity (15,16). The Zn-DPA receptors are metal-organic complexes that have high affinity for phosphate-containing molecules such as siRNA through specific interactions between the coordinated zinc ions of the DPA and the anionic phosphate moieties (17-19). Various Zn-DPA analogues have been developed as useful tools for the sensing of biologically important phosphate derivatives (20-22). However, the application of Zn-DPA analogues for siRNA delivery has not been fully explored. Furthermore, these Zn-DPA analogue-based nanoparticle systems are significantly less cationic in character than conventional siRNA delivery carriers and therefore, have tremendous potential for the development of non-toxic and efficient therapeutic siRNA carriers.

As a nanocarrier for siRNA delivery, multi-functional gold nanorod particles are attractive hybrid materials composed of an inorganic metallic gold core surrounded by an organic or biomolecular layer. These nanomaterials are promising candidates in drug delivery owing to their tunable core size, monodispersity, low toxicity, unique dimensions and tunable surface functionalities as well as the ability for photoacoustic tomography (PAT) (23-26). Especially because of their large surface-to-volume ratio, GNRs are ideal nanocarriers which can provide sufficient surface area for coupling Zn-DPA receptors to complex with siRNA. Furthermore, application of thermotherapy to destroy specific cells is a well-known strategy for the treatment of cancer since it is a noninvasive method and a relatively painless treatment for patients (27-29). Due to the GNRs' strong plasmonic resonance peak, GNRs efficiently convert light energy into surface-localized heat generated as a consequence of electron phonon collisions, known as photothermal conversion, when the near-infrared light matches the plasmon resonance wavelength (30, 31). Heat transfer from the surface of GNRs to the surrounding cellular environment is highly localized, decaying exponentially within a few nanometers and therefore is thought to minimize adverse effects on normal cells (32).

Thus, these properties would reduce damages to healthy cells during photothermal therapy of the tumor region and provide synergistic effect associated with combination therapy of siRNA agents and

photothermal therapy, which will lead to enhanced anti-tumor efficacy. Although single-arm treatment is still widely used for many different cancers, this conventional method remains less effective than combination therapy (33). For the successful cancer treatment, combination therapy is an emerging potential method that combines two or more different therapeutic drugs or treatments by working in a synergistic or additive manner (34). Moreover, this combination therapy requires a lower therapeutic dosage of each individual drug or treatment and could prevent the toxic effects on normal cells while simultaneously producing cytotoxic effects on cancer cells as combination therapy targets different pathways to enhance cytotoxicity to cancer cells. In nanomedicine, the exploitation of multifunctional nanoparticles for effective delivery of combined therapeutic agents or treatments in order to improve cancer therapy has arisen as one of the promising strategies (35, 36).

Polo-like kinase 1 (PLK1) is a member of serine/threonine protein kinases and the most extensively studied member of polo-like kinases. PLK1 has been reported to play a critical role in regulating multiple processes including mitosis, meiosis, spindle assembly, centrosome maturation, anaphase promoting complex (APC), and cytokinesis (37, 38). It has been found that the concentration and activity of PLK1 is important for the processes of cell cycle (39, 40). In addition, PLK1 has also been regarded as a proto-oncogene that is overexpressed in several different cancers, including prostate cancer, breast cancer, and non-small-cell lung cancer, being often correlated with poor patient prognosis while its expression level in normal tissues is often very low or undetectable (41-44). Preclinical studies indicate that pharmacological or genetic inhibition of PLK1 triggers mitotic arrest and enhances cell death in cancer cells. Notably, high expression level of PLK1 in tumors is correlated with low survival rate of patients (42, 45). Recently, numerous inhibitors of PLK1 have been developed to treat several types of cancers (46-50). Thus, PLK1 inhibition is a promising therapeutic approach for cancer therapy.

Herein, we developed a novel nanoformulation by conjugating Zn-DPA (ZD) onto gold nanorods (GNRs) and, subsequently, loading the particle with siRNA. The resulting particles facilitate the release of entrapped siRNA within tumor cells and cause a prominent gene silencing effect. Moreover, due to the unique photoacoustic (PA) property of GNRs, ZD-GNR serves as a theranostic agent for simultaneous PA imaging and therapy of cancer by generating heat upon laser irradiation. Figure 1 illustrates the process of developing siRNA

complexed Zn-DPA conjugated GNRs (siRNA/ZD-GNRs) and working principle of combination therapy of both gene-silencing of siRNA and photothermal effect upon laser irradiation.

## Results and Discussion

### Fabrication and characterization of siRNA/ZD-GNRs

Figure 1 illustrates the process of developing siRNA complexed Zn-DPA conjugated GNRs (siRNA/ZD-GNRs) and working principle of combination therapy of both gene-silencing of siRNA and photothermal effect upon laser irradiation. For the fabrication of siRNA/ZD-GNRs, we coupled

lipoic acid-functionalized bis-DPA molecules onto the surface of gold nanorods (GNRs). First, lipoic acid-modified bis-DPA was synthesized and confirmed by  $^1\text{H-NMR}$  and LCMS (Figure S2 and Figure S3 in the Supporting Information). Second, the DPA-GNRs were synthesized through a ligand exchange reaction that allows replacing hexadecyltrimethylammonium bromide (CTAB) with lipoic acid-modified bis-DPA by forming covalent Au-S bonds between the CTAB-stabilized GNRs and lipoic acid-modified bis-DPA (51). Excess lipoic acid-modified bis-DPA was removed using repeated centrifugation and dispersed in distilled water.

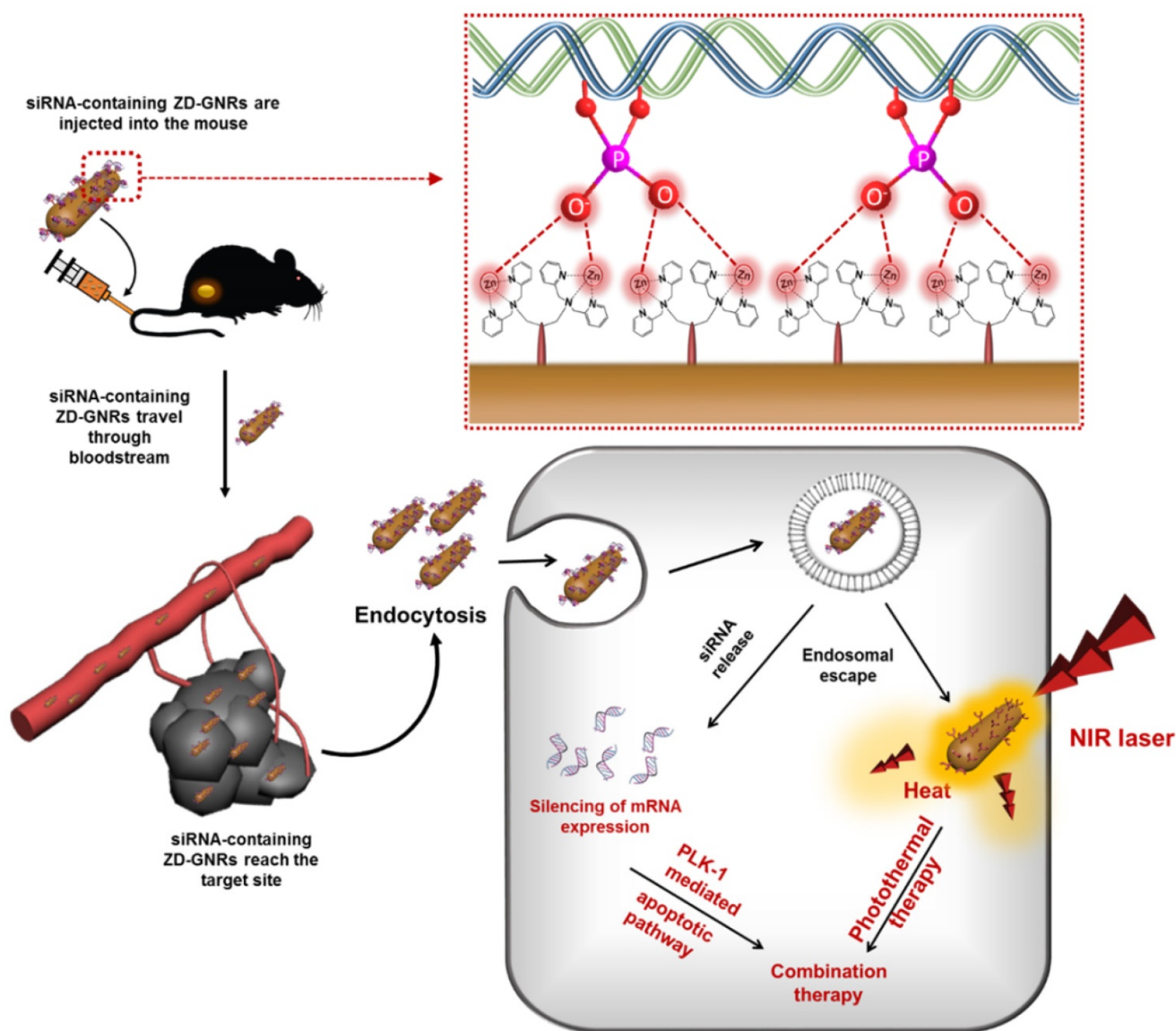


**Figure 1.** Schematic illustration of specific interaction between the Zn(II)-dipicolylamine (Zn-DPA) and phosphate groups of siRNA and combined anti-PLK1 gene therapy/photothermal therapy upon laser irradiation after the accumulation of siPLK1/ZD-GNRs at the target tumor tissues.

To find the ideal molar ratio of [DPA]/[GNRs] and obtain uniform and stable bis-DPA functionalized GNRs, we investigated the conversion of bis-DPA (%) from various molar ratios of [DPA]/[GNRs]. As can be seen in Table S1 in the Supporting Information, we found that low molar feed ratios of [DPA] to [GNRs], such as 10:1 (DPA-GNR1), 50:1 (DPA-GNR2), or 100:1 (DPA-GNR3), resulted in particle aggregation, despite high incorporation of bis-DPA. At the molar feed ratio of 500:1 (DPA-GNR4), we obtained uniform, non-aggregated bis-DPA functionalized GNRs, as demonstrated by transmission electron microscopy (TEM) (Figure 2c). Additionally, the high density of

DPA attached to the GNR surface is expected to have a high affinity for siRNA by specific interactions between coordinated zinc ions of DPA and anionic phosphates of the RNA. Dynamic light scattering (DLS) was employed to characterize the particle size and zeta potential of siRNA/ZD-GNRs and the intermediates. After DPA-GNRs were complexed with zinc ion, the mean diameter of DPA-GNRs slightly increased from  $48.6 \pm 6.8$  to  $51.13 \pm 5.2$  nm and the surface charge decreased but remained positive from  $66.2 \pm 3.4$  to  $24.5 \pm 5.2$  mV due to the complexation of zinc ions with the bis-DPA molecules (Figure 1 and 2b).

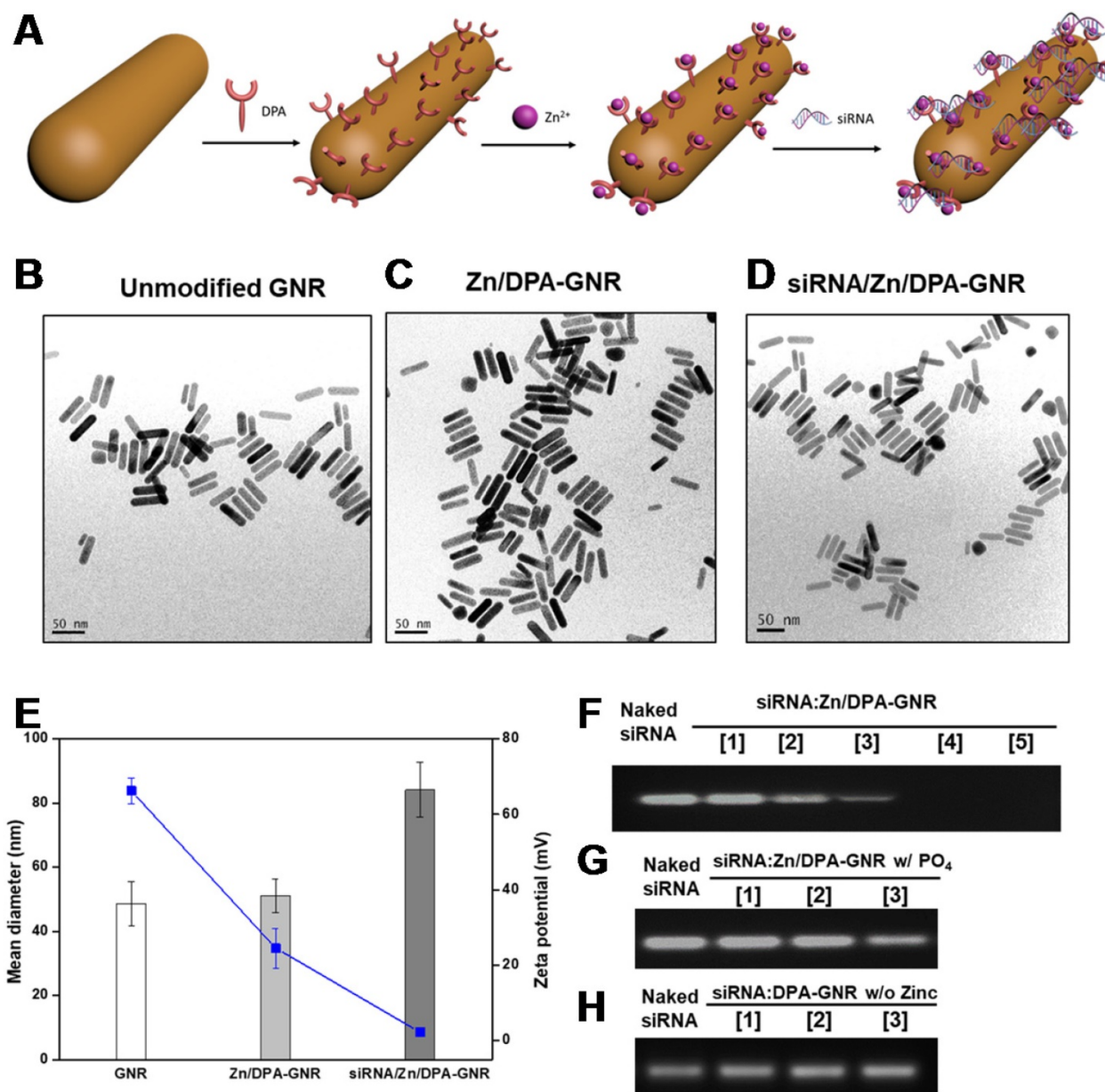


**Figure 2. Characterization of siRNA/ZD-GNRs.** (a) Schematic illustration of assembly of siRNA/ZD-GNRs. (b-d) Representative TEM images of GNRs (b), ZD-GNRs (c), and siRNA/ZD-GNRs (d). (e) Size distribution and zeta-potential of GNRs, ZD-GNRs and siRNA/ZD-GNRs (n = 3). (f-h) Electrophoretic retardation analysis of siRNA binding with ZD-GNRs: (f) (Lanes 1-5: complexes at siRNA/ZD-GNR molar ratios of 600, 300, 200, 100, and 50); (g) After addition of phosphate ions (Lanes 1-3: complexes at molar ratio of 200, 100, and 50); and (h) siRNA binding with DPA-GNRs without zinc ions (Lanes 1-3: complexes at molar ratios of 200, 100 and 50).

The formation of siRNA/ZD-GNR complexes (siRNA/ZD-GNR) was investigated by the agarose gel retardation assay by using a siRNA (siLuc) that targets firefly luciferase (fluc) gene as a model siRNA. When the molar ratio of siRNA/ZD-GNR reached 100, the ZD-GNRs completely bound siRNA to form nano-complexes (Figure 2f). After formulation of siLuc/ZD-GNRs, the complexes formed spherical structures with an average hydrodynamic diameter of  $84.1 \pm 8.6$  nm (Figure 2d, 2e). As seen from Figure 2e, the zeta potential of the siLuc/ZD-GNR complexes decreased to  $2.3 \pm 1.0$  mV due to the complexation of negatively-charged phosphate molecules of siRNA onto the ZD-GNRs. To confirm that the siLuc/ZD-GNR complexes were based on coordination between the zinc ions with DPAs and phosphate molecules of siRNA, the complexation between DPA-GNR and siRNA without zinc ions as well as decomplexation of siLuc/ZD-GNR after the addition of sodium phosphate were investigated in a retardation test (Figure 2g, 2h). As shown in Figure 2h, without zinc ions, ZD-GNRs did not complex with siRNA at any concentration. Furthermore, the compact coordination of siRNA with Zn/DPA ligands was disrupted after the addition of phosphate ions whereas other salts (e.g. NaCl, MgCl<sub>2</sub>) did not affect the siLuc/ZD-GNR complexes (Figure 2g and Figure S4 in the Supporting Information). These results demonstrated the strong and selective binding of phosphate molecules of siRNA with Zn/DPA on the surface of GNRs.

### Cellular uptake and intracellular distribution of siRNA/ZD-GNRs

Cellular uptake of siRNA/ZD-GNRs was examined in 143B cancer cells by dark-field microscopy. As shown in Figure 3a, 143B cells treated with both ZD-GNRs and siRNA/ZD-GNRs for 3 h displayed a strong golden color, suggesting that GNR-based nano-complexes had been taken up by the cells and were located within the cytosol. In order to provide additional evidence of intracellular distribution, Cy3-siRNA/ZD-GNRs, Cy3-siRNA/LipoMax and free Cy3-siRNA were incubated with 143B cancer cells (Figure 3b and Figure S5 in the Supporting Information). The intracellular fluorescence signals of siRNA/ZD-GNRs in 143B cancer cells were monitored by confocal laser scanning microscopy (CLSM). After 1 h incubation, 143B cells with Cy3-siRNA/ZD-GNRs exhibited a strong and bright red fluorescence in the cytosol. This indicated the uptake of the nanoparticles into the cells and their location at the endo/lysosomal compartments in the cytosol. After 3 h incubation of 143B cells with Cy3-siRNA/ZD-GNRs, the red

fluorescence was broadly found and evenly distributed within the cytosol, which can be ascribed to the released siRNA from internalized siRNA/ZD-GNRs. Interestingly, it was found that intracellular distribution using Cy3-siRNA/LipoMax showed a similar uptake pattern compared to siRNA/ZD-GNRs. In contrast, 143B cells treated with free Cy3-siRNA exhibited a negligible red fluorescence within the cytosol due to the difficulty of cell permeation of large, negatively charged siRNA molecules. The mechanism regarding endosomal escape of siRNA/ZD-GNRs may be due to proton sponge effect (23, 52). Because the zinc ion or pyridine molecule of DPA or ZD-DPA would complex with chloride, protons or anions such as pyrophosphate, ADP and ATP, respectively, inducing the entering of water molecules to the lysosome. This process results in swelling and rupture of lysosome, with siRNA/ZD-GNRs released into the cytosol. However, the detailed mechanism remains elusive. Collectively, these results imply that siRNA/ZD-GNRs can be localized within endo/lysosomes and effectively internalized within cells after escaping from endo/lysosomes and eventually siRNA can be released from the complexes, such as the mechanism of Lipomax, for siRNA delivery<sup>42-44</sup>.

### In Vitro Gene Silencing Effect of siRNA/ZD-GNRs

An ideal siRNA delivery nanoparticle must traffic its siRNA payload successfully from endo/lysosomes into the cytosol where the siRNA must exhibit gene silencing effects. The degree of gene silencing by siLuc/ZD-GNRs was examined in 143B-fluc cells using bioluminescence imaging (BLI). Luciferase activity was measured in cells treated with free siLuc, siLuc/LipoMax, siLuc/DPA-GNRs without zinc ions, negative control siRNA (siNC) with ZD-GNRs (siNC/ZD-GNRs), and siNC/LipoMax. As expected from a cellular uptake study in Figure 2b, free siLuc did not display any distinct fluc gene silencing effect at any concentration (Figure S6 in the Supporting Information). Moreover, siLuc/DPA-GNRs without zinc ions, siNC/ZD-GNRs or siNC/LipoMax also did not achieve obvious gene silencing effect in the target cells (Figure 3c, d and Figure S6 in the Supporting Information). In particular, a remarkably high gene silencing efficacy in cells treated with siLuc/ZD-GNRs was found in a dose-dependent manner (Figure 3c,d). As the concentration of siRNA increased, the expression of fluc from the 143B cells was reduced to  $84.55 \pm 5.32\%$ ,  $57.60 \pm 2.52\%$ , and  $15.77 \pm 0.55\%$  when 0.625, 2.5, and 10 pmol siLuc/ZD-GNRs were added, respectively. These observations demonstrate that ZD-GNRs, as an

siRNA delivery carrier, can bind to the siRNA molecules by forming compact complexes through specific interactions between coordinated zinc ions of DPA and anionic phosphates of the siRNA, allow its cellular uptake, promote endo/lysosome escape, and finally release siRNA molecules into the cytosol, where unique sequence-specific gene silencing effect occurs.

### Photothermal Properties of the ZD-GNRs

We next investigated the photothermal effect of

the ZD-GNRs. Because the gold nanorods have peak absorbance around 800 nm, 808 nm laser source is suitable for photothermal experiments<sup>45</sup>. Different concentrations of ZD-GNRs were evaluated at fixed laser power (1.0 W/cm<sup>2</sup>) for 10 min. The temperature of the ZD-GNR solution increased in a dose-dependent manner (Figure 4a). The ZD-GNR solution (4 µg/mL) showed rapid temperature increase to about 65 °C within 10 min. As shown in Figure 3b, we also observed temperature change of ZD-GNRs at a fixed concentration (2 µg/mL) and

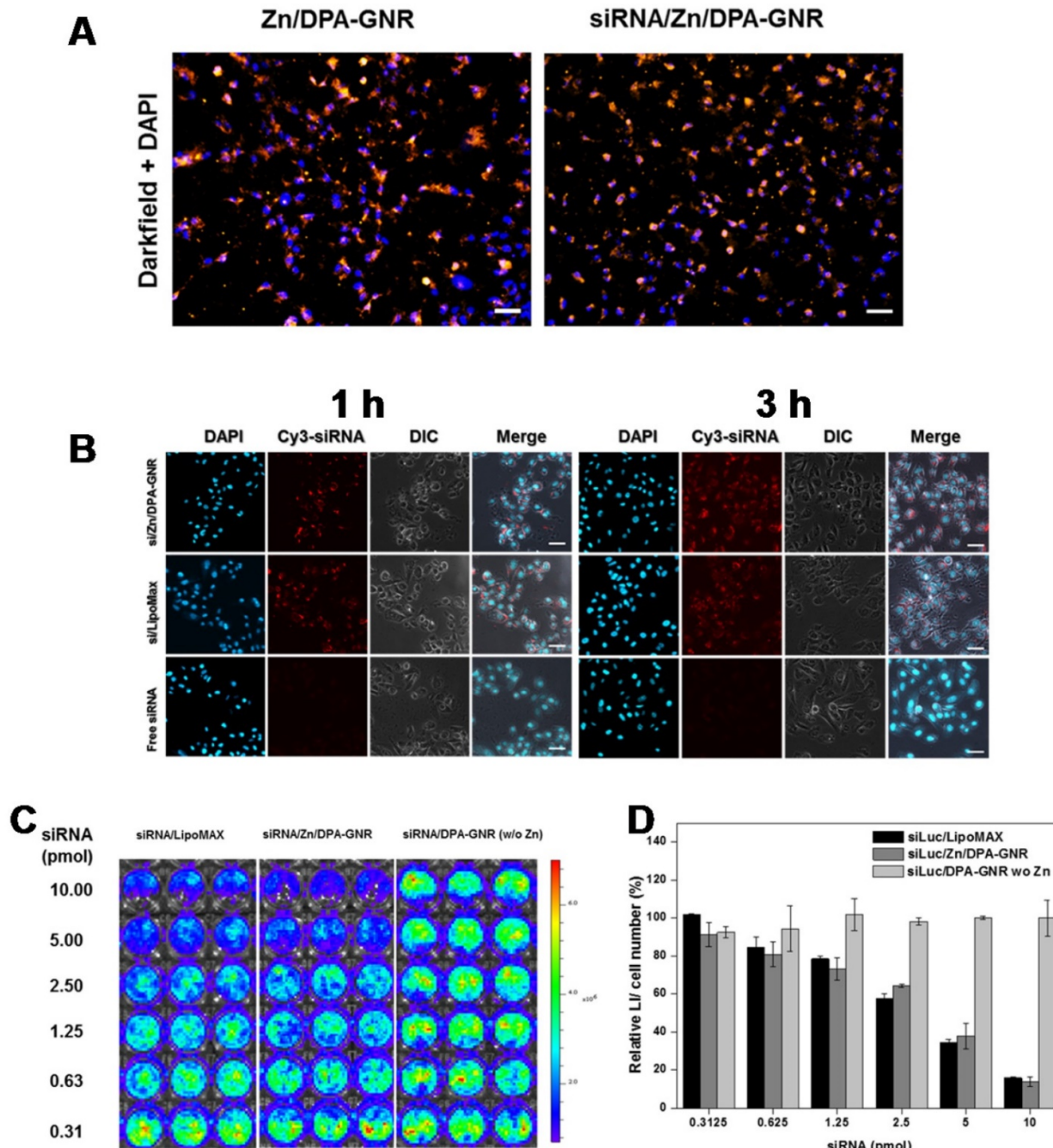


**Figure 3.** (a) Dark-field light scattering and DAPI images of ZD-GNRs and siRNA/ZD-GNRs after incubation with 143B cells for 3 h. (b) CLSM images of 143B cells treated with Cy3-labeled siRNA/ZD-GNRs for 1 and 3 h. (c-d) Suppression of fLuc gene expression of 143B-fLuc cells after treatment with siLuc/LipoMax, siLuc/ZD-GNRs or siLuc/DPA-GNRs without zinc ions. Scale bar: 20 µm.

irradiated with different laser powers, which showed laser-power-dependent temperature increase. More importantly, to confirm the photothermal properties of ZD-GNRs after being taken up by cells, 143B cells were treated with ZG-GNRs for 5 h and the medium was washed twice and replaced with fresh medium. The temperature change of GD-GNRs in cell culture medium was monitored upon laser irradiation. The cell culture without particles showed almost no heating effect. However, the Zn-GNR treatment (2  $\mu\text{g}/\text{mL}$ ) followed by 1.0  $\text{W}/\text{cm}^2$  laser treatment raised the medium temperature by about 30  $^{\circ}\text{C}$  within 10 min (Figure 3c), which is high enough for cell killing.<sup>46</sup> Taken together, the results above confirmed that the siRNA/ZD-GNRs can effectively deliver siRNA into cells, silence target genes, and have photothermal effect by gold nanorods upon laser irradiation.

### In Vitro Combination Treatment with Gene and Photothermal-therapy

To demonstrate the potency of siRNA/ZD-GNRs for combination therapy of cancer, we chose polo-like kinase 1 (PLK1), a serine/threonine protein kinase which plays a critical

role in mitosis as a therapeutic target.<sup>34-36</sup> The RT-PCR analysis showed that PLK1 mRNA was abundant in three types of prostate carcinoma cell lines including PC-3, DU145, and LNCaP, but was negligible in normal MCF10A cells (Figure S7 in the Supporting Information). After confirming the successful cell uptake of ZD-GNRs and siPLK/ZD-GNRs by using ICP-OES analysis (Figure S8 in the Supporting Information), we first investigated the cytotoxicity of siPLK/ZD-GNRs on these prostate carcinoma cell lines.

The siRNA-free ZD-GNRs showed negligible cell death on all three cell lines for concentration up to 50  $\mu\text{g}/\text{mL}$  and 48 h treatment (Figure S9 in the Supporting Information). Moreover, there is no obvious damage to the cells treated with negative control siRNA loaded GNR formula (siNC/ZD-GNRs) for siRNA concentration up to 20 pmol (Figure S10 in the Supporting Information). As shown in Figure S11 in the Supporting Information, the silencing PLK1 by siPLK/ZD-GNR nanocomplex decreased the viability of cancer cells in a dose-dependent manner.

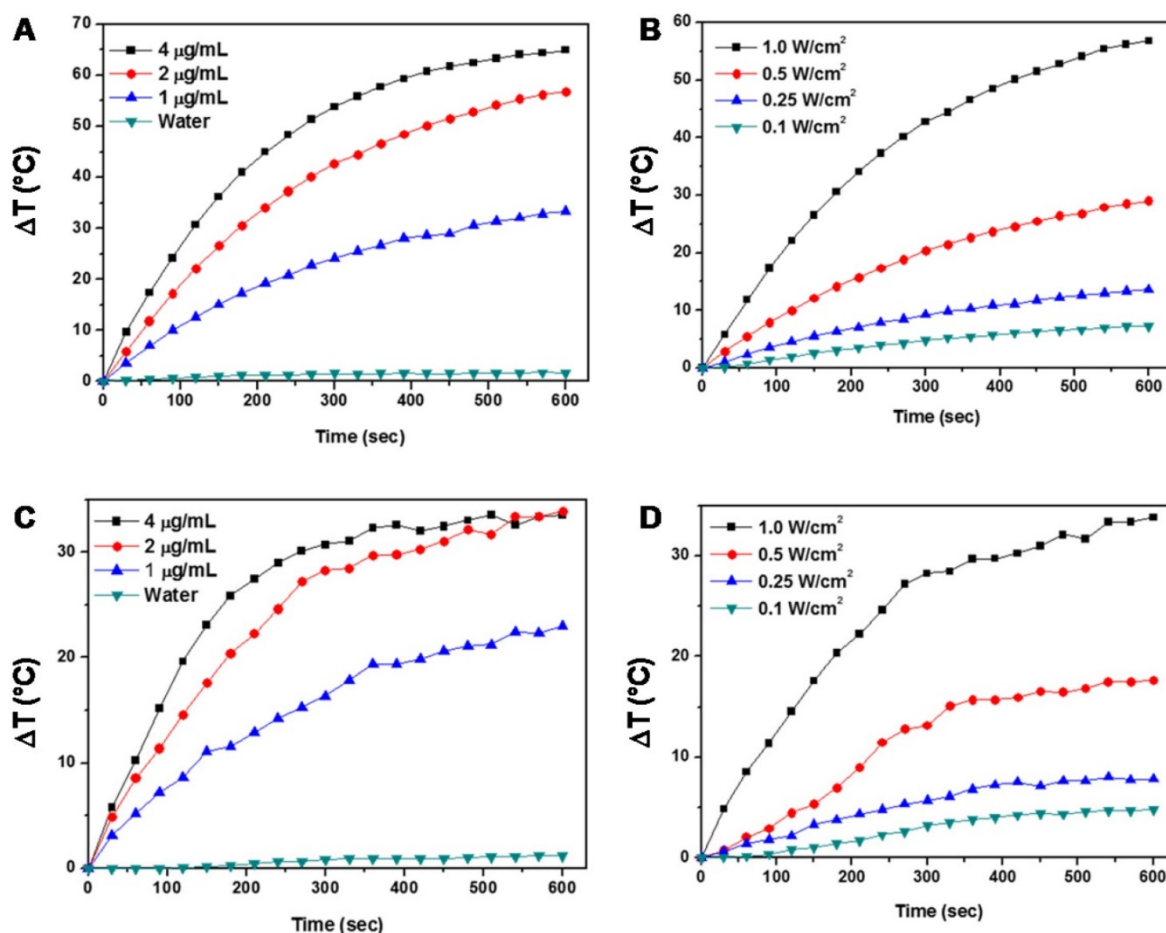


**Figure 4. Photothermal studies of ZD-GNRs.** (a-b) Temperature changes of ZD-GNRs at different concentrations irradiated with an 808 nm laser at power density of 1.0  $\text{W}/\text{cm}^2$  (a) and with different laser powers at a fixed concentration (2  $\mu\text{g}/\text{mL}$ ) (b). (c-d) Temperature variation of 143B cells treated with ZD-GNRs in culture medium at different concentrations irradiated with an 808 nm laser at power density of 1.0  $\text{W}/\text{cm}^2$  (c) and with different laser powers at a fixed particle concentration (2  $\mu\text{g}/\text{mL}$ ) (d).

Next, combined gene and photothermal therapy of siPLK/ZD-GNRs was conducted. The prostate cancer cells were incubated with siPLK/ZD-GNRs, ZD-GNRs, or PBS for 24 h and 48 h. After being washed and placed in fresh cell culture medium, the cells with and without 808 nm laser irradiation were examined by a cell counting kit-8 (CCK-8) assay. As shown in Figure 5a and b, siPLK/ZD-GNRs with laser irradiation produced significantly higher cytotoxic effect against PC-3 cells than ZD-GNRs only with laser or siPLK/ZD-GNRs without laser. Similar results were also seen for DU145 and LNCaP cells (Figure S12a, b and S13a,b in the Supporting Information). The cytotoxicity of siPLK/ZD-GNRs was further evaluated using Annexin V-FITC and PI staining (Figure 5c, d), which distinguishes non-apoptotic cells (no fluorescence), early apoptotic cells (green fluorescence), necrotic cells (red fluorescence) and late apoptotic and necrotic cells (green and red fluorescence)<sup>47</sup>. In the case of siPLK/ZD-GNRs only without laser, the cells showed prominent green fluorescence due to early apoptosis induced by PLK1 depletion at day 1 and weak red fluorescence because of the presence of a small number of late apoptotic and necrotic cells at day 2. When PC-3 cells were incubated with siPLK/ZD-GNRs followed by laser irradiation, both green and red fluorescence appeared, showing the efficacy of combination therapy of PLK1 depletion and PTT induced apoptosis and necrosis in cancer cells. Notably, even though treatment with ZD-GNRs and laser irradiation also induced apoptosis and necrosis, siPLK/ZD-GNRs with laser led to the highest extent of apoptosis and necrosis. Similar results were also found from the FACS analysis (Figure 5e,f). The combination therapy was also highly effective for DU145 and LNCaP cells (Figure S12c-f and S13c-f in the Supporting Information). Moreover, mRNA level of PLK1 was also evaluated using reverse transcription polymerase chain reaction (RT-PCR) (Figure S14 in the Supporting Information), manifesting the effectiveness of gene silencing by siPLK/ZD-GNRs.

### **In Vivo Photoacoustic Imaging of siPLK/ZD-GNRs**

Photoacoustic imaging (PAI) is recognized as a promising imaging tool with high contrast and spatial resolution to investigate distribution and accumulation of metallic particles such as gold in target tumor tissue<sup>48</sup>. Before performing the gene and photothermal combination therapy, PAI of siPLK/ZD-GNRs was monitored in PC-3 tumor-bearing mice. When the tumor volume reached  $\sim 100 \text{ mm}^3$ , the mice were treated by an intravenous

injection of the siPLK/ZD-GNRs (100  $\mu\text{L}$  in saline, 0.1 mg/mL). As shown in Figure 6, after treatment with siPLK/ZD-GNRs, the PA signal in the tumor region gradually increased with time and the PA intensity at 24 h was 6.0 times higher than that before injection. Additionally, the 3D-PAI images showed remarkably strong intensity in the tumor region at 24 h post-injection, indicating excellent tumor accumulation of siPLK/ZD-GNRs, which was also confirmed by biodistribution of gold content (Figure S15 in the Supporting Information).

### **In Vivo Combined Gene and Photothermal Therapy**

Before the *in vivo* therapeutic experiment, we first performed the serum stability of the siPLK/ZD-GNRs because serum nuclease attack in bloodstream is one of major challenges for systemic delivery of siRNA.<sup>(53)</sup> When serum stability was examined in the 40% fetal bovine serum (FBS) solution at 37 °C, the free siRNA was broken down within 12 h incubation, whereas siPLK/ZD-GNRs were stable to serum solution even after 24 h incubation (Figure S16 in the Supporting Information). These results indicate that siPLK/ZD-GNRs are stable from nuclease attack in the bloodstream when performing *in vivo* combination treatment because of their strong complexation. Based on the excellent *in vitro* therapeutic behavior and *in vivo* tumor accumulation of siPLK/ZD-GNRs, this nanoplatform was investigated for anti-tumor efficacy on PC-3 tumor-bearing mice. Free ZD-GNRs and the siPLK/ZD-GNRs were administered intravenously when the tumor volume reached  $\sim 100 \text{ mm}^3$ . At 24 h post-injection, the tumors were irradiated with 808 nm laser at a 0.5 W/cm<sup>2</sup> laser power for 10 min and the temperature increase was monitored using an infrared thermal camera for *in vivo* thermal imaging. As shown in Figure 6a,b, no obvious temperature change was observed in the saline group. In contrast, both ZD-GNRs and siPLK/ZD-GNRs treated mice displayed an increase of  $\sim 21 \text{ }^\circ\text{C}$  in the tumor region, which is high enough to ablate the tumor tissue<sup>49</sup>. Figure 6c shows the changes in PC-3 tumor volumes in nude male mice after intravenous injection of saline with or without laser irradiation, the ZD-GNRs with or without laser irradiation, and the siPLK/ZD-GNRs with or without laser irradiation. The control groups (saline with or without laser irradiation, ZD-GNRs without laser irradiation) did not show any substantial delay of tumor growth. The treatments with siPLK/ZD-GNRs without laser irradiation or ZD-GNRs with laser irradiation were effective in delaying tumor growth but not tumor regression. The

siPLK/ZD-GNRs with laser irradiation is the most efficacious in tumor reduction compared to all the other study groups (Figure 6c,d). Moreover, it was found that the expression of PLK1 was significantly down-regulated in the siPLK/ZD-GNRs with laser irradiation group, indicating that the combination treatment induced the apoptosis of target tumor tissues (Figure S17 in the Supporting Information). At the end of the *in vivo* experiment, the PC-3 tumor tissues were dissected from tumor-bearing mice and weighed, which was consistent with the tumor's volume measured by a caliper (Figure 6e). We also investigated the body weight for the possible *in vivo* systemic toxicity of siPLK/ZD-GNRs with or without laser irradiation, and no significant body weight change was found in any of the treatment group. Altogether, the improved antitumor efficacy of siPLK/ZD-GNRs with laser irradiation can be explained by the synergy of combined systemic gene silencing induced apoptosis and locally focused photothermal therapy.

## Conclusions

We successfully developed siRNA-complexed Zn(II)-DPA conjugated gold nanorods (siRNA/ZD-GNRs) through an artificial siRNA receptor, Zn(II)-DPA, which can strongly bind siRNA molecules for combined gene and photothermal tumor treatment. The introduction of gold nanorods with Zn(II)-DPA as a siRNA delivery carrier provided not only sufficient complexation with siRNA in the form of stable nanoparticles, which show strong gene-silencing activity, but also photothermal property of GNRs upon laser irradiation. Moreover, the application of siPLK/ZD-GNRs for gene/photothermal combination therapy demonstrates synergistic antitumor efficacy, which is significantly better than individual gene therapy or PTT alone. Additionally, due to the photoacoustic character of GNRs, siRNA/ZD-GNRs have great potential as a theranostic agent for simultaneous PA imaging and therapy of cancers. The approach suggested in this work may provide a valuable general strategy for efficient combination treatment of cancer.

## Materials and Methods

The synthetic schemes and experimental details are described in the Supporting Information section. All animal experiments were conducted in accordance with a protocol approved by the CC/NIH ACUC committee.

### Materials

CTAB-stabilized GNRs were purchased from

Nanopartz Inc. (Loveland, CO). Cells were purchased from the American Type Culture Collection (Rockville, MD). Other chemicals and biological materials were obtained from Sigma-Aldrich (St. Louis, MO) or Invitrogen (Carlsbad, CA). All the siRNAs were synthesized by Thermo Fisher Scientific (Waltham, MA). The sequences of siRNA firefly luciferase (siLuc) are 5'-GCACUCUGAUUGACAAA UACGAUUU-3' (sense) and 5'-AAAUCGUAUUUGU CAAUCAGAGUGC-3' (antisense), the sequences of siRNA negative control (siNC) are 5'-AAUUCUCCGAACGUGUCACGU-3' (sense) and 5'-ACGUGACACGUUCGGAGAAU-3' (antisense), and the sequence of siRNA targeting Plk1 mRNA (siPLK) are 5'-UGAAGAAGAUCACCCUCCUUA dT-3' (sense) and antisense strand, 5'-UAAGGAGGG UGAUCUfUCUfUCfAdTdT-3' (antisense).

### Synthesis of DPA-GNRs

To prepare gold nanorods modified with dipicolylamine (DPA-GNRs), DPA-GNRs was synthesized by a ligand exchange reaction between CTAB-stabilized GNRs and lipoic acid-modified DPA. The lipoic acid-modified DPA in ethanol (2 mL) was slowly added to the 10 mL of CTAB-stabilized GNRs (2 nM) colloid, and the solution was kept at room temperature for 12 h. The DPA modified GNR (DPA-GNR) solution was centrifuged 3 times at 6000 rpm to remove unreacted lipoic acid-modified DPA species from 6 mL of ethanol/distilled water (1:5, v/v) and dispersed in 2 mL of distilled water. To determine the conversion of DPA and composition ratio, the unreacted lipoic acid-modified DPA in the supernatant was collected and the concentration was determined by measuring the UV absorbance intensity at 350 nm.

### Formulation of siRNA/ZD-GNRs

siRNA/ZD-GNRs were prepared by a metal-organic complex technique. DPA-GNRs at 2 mg/mL were dispersed in ultrapure water (UPW) for 30 min and then 5 mL of 10 mM zinc nitrate hexahydrate was mixed with 5 mL of DPA-GNRs (2 mg/mL in UPW). The resulting mixture was incubated at room temperature for 30 min. After centrifugation (5000 rpm, 3x) to remove excess zinc, ZD-GNR were dispersed in UPW. At the molar ratio of 100 the ZD-GNR dispersion (2  $\mu$ L, 0.1  $\mu$ M) was mixed with 1  $\mu$ L of siRNA (20  $\mu$ M) (siRNA against firefly luciferase (siLuc) or siRNA against PLK1 (siPLK)), and incubated at room temperature for 30 min. The siRNA/ZD-GNRs were then kept at 4 °C for *in vitro* or *in vivo* applications.

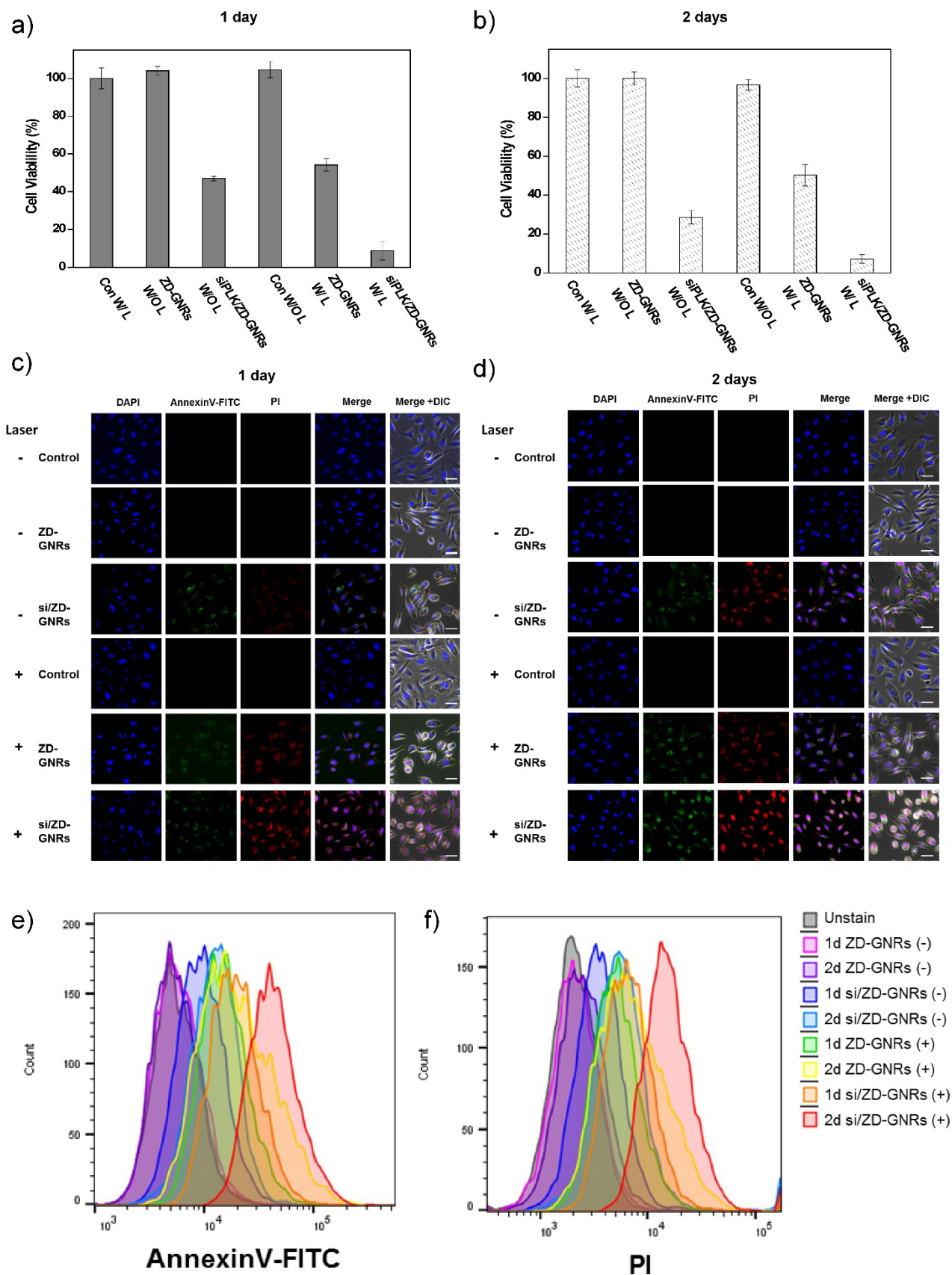


**Figure 5.** *In vitro* combinational gene/photothermal therapy of PC-3 cells with siPLK/ZD-GNRs. (a-b) *In vitro* cytotoxicity of saline, ZD-GNRs, and siPLK/ZD-GNRs with and without 808 nm laser irradiation at power density of 0.5 W/cm<sup>2</sup> against prostate cancer cells after incubation for 1 day (a) and 2 days (b). (c-d) Confocal microscopy images of PC-3 cells treated with PI and Annexin V (AV) after treatment after incubation for 1 day (c) and 2 days (d) (Blue fluorescence is associated with DAPI; the green fluorescence is expressed by Annexin V-FITC, and the red fluorescence is released from PI). (e-f) Scale bar: 20 μm. Flow cytometry data of PC-3 cells treat with PI and Annexin V (AV) after treatment after incubation for 1 day (e) and 2 days (f).

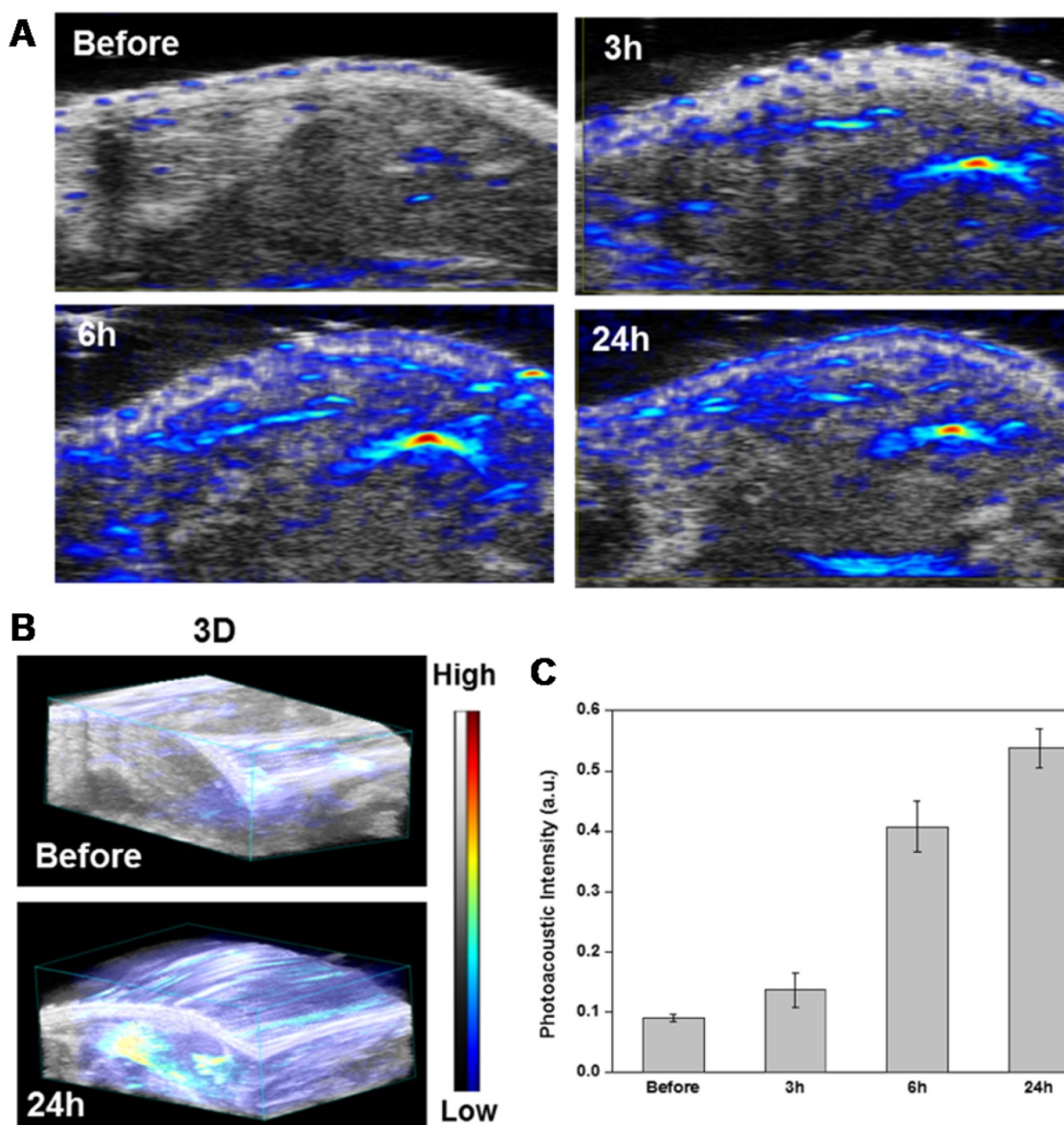


**Figure 6.** *In vivo* photoacoustic imaging of siPLK/ZD-GNRs. (a-b) 2D images (a) and 3D images (b) of the PC-3 tumor region at different time points after intravenous injection of siPLK/ZD-GNRs. (c) histogram of PA intensity profile of the tumor as a function of time.

### Agarose Gel Electrophoresis

siRNA/ZD-GNRs were evaluated by agarose gel retardation assay. The gels were prepared with 2% agarose in Tris-acetate-EDTA buffer containing 0.5  $\mu\text{g}/\text{mL}$  ethidium bromide and 2 mM of zinc ion. Twenty microliters of complexes containing solution with 1  $\mu\text{g}$  siRNA was electrophoresed with Tris-acetate-EDTA (TAE) running buffer. Gel electrophoresis was carried out at 100 V for 30 min and the gel was imaged using a LAS-3000 gel documentation system (Fujifilm Life Science, Japan). To assess the decomplexation of siRNA, siRNA/ZD-GNRs were incubated with 0.1 M sodium phosphate, sodium chloride or magnesium chloride

for 30 min and the released siRNA fraction was imaged.

### Inductively Coupled Plasma Emission Spectrometry (ICP-OES)

Quantification of siRNA/ZD-GNRs taken up in cells was performed using ICP-OES. Prostate cancer cells seeded onto a 6-well plate were incubated for 24 h and then treated with ZD-GNRs (3  $\mu\text{g}/\text{mL}$ ) or siRNA/ZD-GNRs (3  $\mu\text{g}/\text{mL}$ ) for another 24 h. Cells were then harvested and digested by 200  $\mu\text{L}$  of aqua regia. 50  $\mu\text{L}$  of ZD-GNRs were also digested in 100  $\mu\text{L}$  of aqua regia. The digested samples were diluted with ultrapure water to 5 mL and the gold concentration was measured by ICP-OES (Agilent 700 Series, Santa Clara, CA).

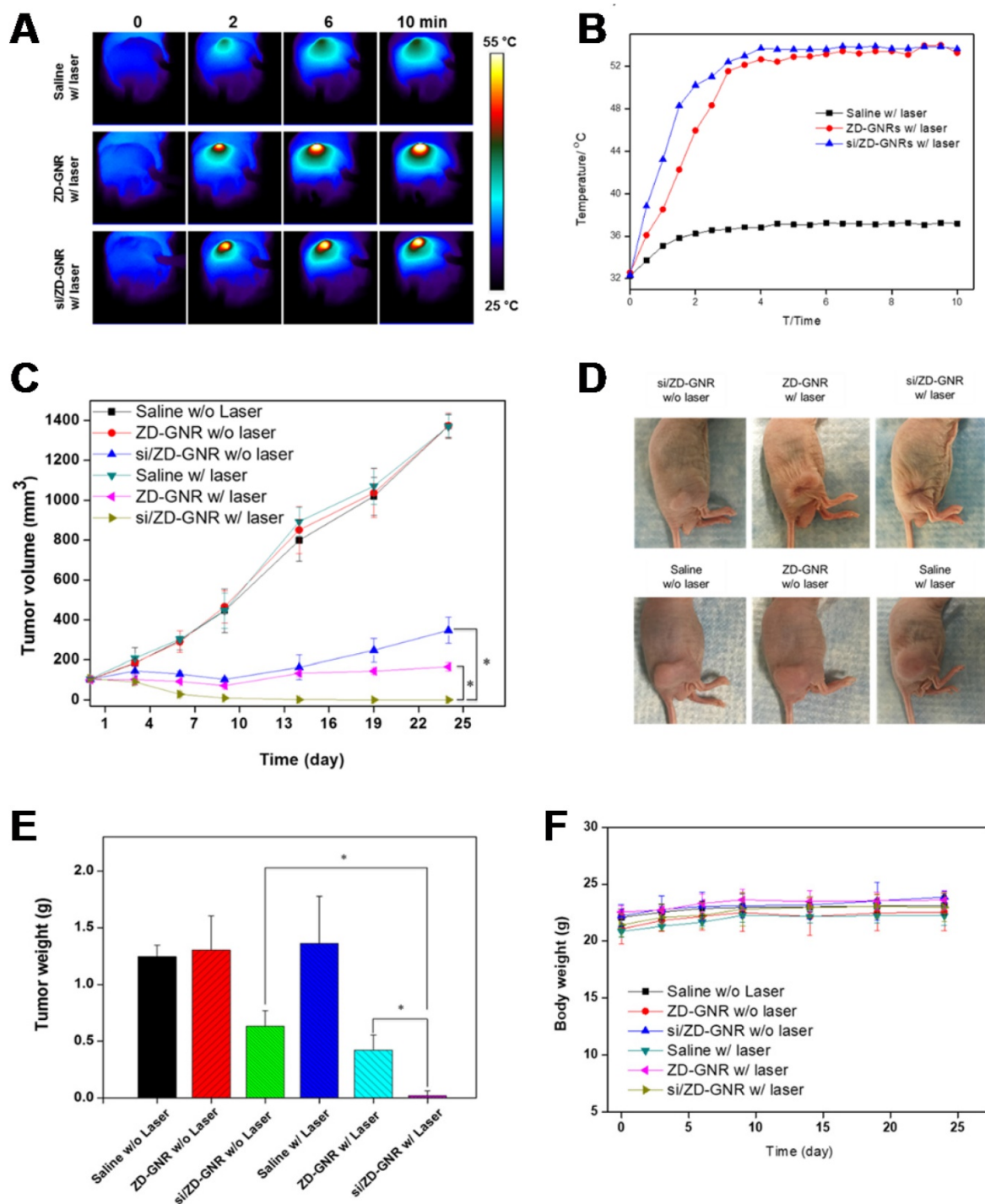


**Figure 7. Combinational gene/photothermal therapy of siPLK/ZD-GNRs on PC-3 tumor-bearing mice.** (a-b) Thermographic images (a) and temperature changes of the tumor area (b) of the mice treated with saline, ZD-GNRs, and siPLK/ZD-GNRs upon 10 min laser exposure. (c) Changes in tumor volumes after intravenous injection of the samples with or without laser exposure. (d) Representative images of PC-3 tumor-bearing mice at day 23 after treatment. (e) Weights of excised tumors (n = 4/group). (f) Body weight of tumor-bearing mice after treatment. (\*P < 0.05).

### Gene Silencing Effects of siRNA/ZD-GNRs in Cells

143B cells stably expressing firefly luciferase (fluc) reporter gene were maintained in MEM medium with 10% FBS at 37 °C in a humidified 5% CO<sub>2</sub> atmosphere. To confirm gene silencing effect of siRNA/ZD-GNRs, 143B cells were seeded in 96-well

plates and treated with siLuc/ZD-GNRs (8 μL; 10 pmol siRNA) dispersed in 92 μL of cell culture medium. Parallel experiments for positive control (siLuc/LipoMAX) and negative control (siNC/ZD-GNRs or siNC/LipoMAX) were also carried out. After 24 h incubation, the fLuc level was quantified using a bioluminescence imaging system (Xenogen

IVIS-100).

### Darkfield Light Scattering Imaging

Darkfield images were taken with a Zeiss Axioskop 2 plus microscope equipped with a black-white CCD camera. All images were taken at 60X magnification under the same lighting conditions using an Olympus IX-81 inverted epifluorescence microscope.

### In Vitro Confocal Microscopy Imaging

143B cells were seeded onto coverslip-bottom culture chambers (LabTEK) in 200  $\mu$ L of MEM supplemented with 10% FBS and 1% antibiotics (penicillin 100 U/mM, streptomycin 0.1 mg/mL). After incubation for 24 h (37 °C, 5% CO<sub>2</sub>), the medium was carefully aspirated and replaced with 1 mL of medium containing siRNA/ZD-GNRs. The cells were incubated for 1 and 6 h and then washed three times with PBS. The cells were fixed with 4% w/v formaldehyde for 5 min. Cells were then washed with PBS and mounted with antifade mounting medium with DAPI (Vectashield, Burlingame, CA). Confocal microscopy was performed with an Olympus Fluoview FV10i (Olympus, Tokyo, Japan).

### Measurement of Photothermal Effect of ZD-GNRs

ZD-GNRs were diluted into different concentrations with distilled water. Aliquots of samples were exposed to an 808 nm NIR laser (Laserglow Technologies, Toronto, Ontario, Canada) for 10 min at different power densities. A laser energy meter (Coherent Portland, OR) was used to measure and calibrate the laser densities. The temperature increase of the solutions was recorded with an infrared thermal imaging system (FLIR® Systems, Oregon, USA).

### Measurement of In Vitro Photothermal Effect after Cell Uptake of ZD-GNRs

143B cells ( $3 \times 10^5$  cells/well) were seeded onto 6-well flat-bottomed plates in 2 mL of MEM cell culture medium supplemented with 10% FBS and 1% antibiotics and incubated for 24 h. The medium was aspirated and incubated with various concentrations of ZD-GNRs for 24 h at 37 °C. The cells were washed twice with PBS to remove the remaining ZD-GNRs, and the cells were harvested and resuspended in MEM medium. The samples were exposed to an 808 nm NIR laser for 10 min at different power densities. The temperature changes of the cell culture medium were recorded with an IR thermal camera.

### In Vitro Photothermal Effect of the siPLK/ZD-GNRs Irradiated with an NIR Laser

0.2 mL of siPLK/ZD-GNRs in a 1 mL tube was irradiated with an 808 nm laser at different power densities for 10 min. The spot size of the laser was adjusted to cover the entire solution surface. The thermal images and temperature increase of the aqueous solutions were recorded by using an infrared thermal camera. The water control was also treated under the same conditions.

### Prostate Carcinoma Cell Culture

Three human prostate cancer cell lines, including PC-3, LNCaP and DU145 were used in this study. The PC-3 cells were cultured in F12 (Life Technologies, Carlsbad), LNCaP cells were cultured in RPMI-1640 (Life Technologies, Carlsbad), and DU145 cells were cultured in MEM (Life Technologies, Carlsbad) supplemented with 10% FBS and 1% penicillin-streptomycin (Gibco, Grand Island, NY) in a humidified incubator at 37 °C with 5% CO<sub>2</sub>.

### In Vitro Combined Gene and Photothermal-therapy

Three cancer cells (PC-3, DU145, and LNCaP) were seeded at a density of  $5 \times 10^3$  cells/well in 96-well well plate. After 24 h, the cells were washed twice with PBS and incubated with various concentrations of siPLK/ZD-GNRs, ZD-GNRs for 24 h or 48 h at 37 °C. The cells were then washed with PBS, and 100  $\mu$ L of fresh medium was added. The cells were irradiated with or without an 808 nm laser at a power density of 0.5 W/cm<sup>2</sup> for 5 min, respectively. After incubation for another 2 h, the viability of cancer cells was examined using the standard CCK-8 assay.

### RT-PCR Analysis

The total RNA content was prepared from siPLK/ZD-GNRs treated PC-3, DU145, and LNCaP cell lysates after TRIzol extraction, and then RNA quantity was quantified using a Nanodrop spectrophotometer (Thermo Fisher Scientific, Waltham, MA). To synthesize cDNA, 1  $\mu$ g of RNA was used by Verso cDNA synthesis Kit (Thermo Fisher Scientific, Waltham, MA). The sequences of the forward and reverse primers of PLK1 were 5'-CTGCCTGACCATTCCACCAA and 5'-GTGCCGTCACGCTCTATGTA, respectively. The sequences of the forward and reverse primers of  $\beta$ -actin were 5'-ACAGAGCCTCGCCTTTGC and 5'-AGAGGCGTACAGGGATAGCA, respectively. The PCR reaction (94°C for 30 s, 60°C for 30 s, 72°C for 30 s) was run for 30 cycles after an initial single cycle of 94°C for 2 min to activate the Taq polymerase. For final elongation, single step was performed at 72°C for

15 min. After amplification, PCR products were analyzed by gel electrophoresis in 1.8% agarose gels and visualized by GelRed™ (Biotium, Hayward, CA) staining.

### Serum Stability of siRNA/ZD-GNRs

FBS was mixed with 20  $\mu$ L of complexes containing solution with 1  $\mu$ g siRNA (free siRNA or siRNA/ZD-GNRs) at the final concentration of 40% and then incubated at 37 °C during the indicated period. The samples were then analyzed by agarose gel (2%) under TBE (Tris-borate-EDTA) running buffer. Gel electrophoresis was carried out at 100 V for 30 min and the gel was subsequently imaged using a LAS-3000 gel documentation system (Fujifilm Life Science, Japan).

### In Vivo Photoacoustic Imaging

The PC-3 xenograft tumor was established by inoculating 10 million cells into the right flank of athymic C3H/HeN nude mice (20-25 g, Harlan, Indianapolis, IN). When tumors reached 100 mm<sup>3</sup> in volume, the mice (n = 3) were treated by an intravenous injection of the siPLK/ZD-GNRs (100  $\mu$ L in saline, 0.1 mg/mL). The PA image of the whole tumor region was scanned by using the VisualSonic Vevo 2100 LAZR system (40 MHz, 256-element linear array transducer) at 0, 3, 6, and 24 h postinjection.

### In Vivo Biodistribution by ICP-OES

To study the biodistribution of the particles in various organs, when PC-3 tumors reached a size of 100 mm<sup>3</sup> in volume, 250  $\mu$ L suspension of siPLK/ZD-GNRs was intravenously injected into PC-3 tumor mice. The mice were sacrificed at 3, 6, 12, 24, and 48 h post-injection and organs including tumor, heart, liver, spleen, lung and kidneys were dissected and weighted. Each group had three mice as replicates. All the samples were stored at -80 °C before ICP-OES measurement.

### In Vivo Combined Gene and Photothermal-therapy

When tumors reached a size of 100-150 mm<sup>3</sup> in volume, saline (250  $\mu$ L), saline with laser irradiation (250  $\mu$ L), ZD-GNRs (250  $\mu$ L), ZD-GNRs with laser irradiation (250  $\mu$ L), siPLK/ZD-GNRs (250  $\mu$ L; siRNA 1.5 nmol), and siPLK/ZD-GNRs with laser irradiation (250  $\mu$ L; siRNA 1.5 nmol) were injected intravenously at days 0, 3, and 6 (4 mice/group). At 24 h after the injection of the third dose, the PC-3 tumors were exposed to an 808 nm laser (0.5 W/cm<sup>2</sup>) for 10 min. The body weights of mice were recorded, and tumor volumes were calculated as  $a \times b^2/2$ , where a and b are the largest and smallest diameters, respectively.

### In Vivo Gene Expression Evaluation in Tumor Tissue by RT-PCR

Nude mice bearing PC-3 tumors (100-150 mm<sup>3</sup>) were intravenously injected with saline (250  $\mu$ L), saline with laser irradiation (250  $\mu$ L), ZD-GNRs (250  $\mu$ L), ZD-GNRs with laser irradiation (250  $\mu$ L), siPLK/ZD-GNRs (250  $\mu$ L; siRNA 1.5 nmol), or siPLK/ZD-GNRs with laser irradiation (250  $\mu$ L; siRNA 1.5 nmol) at days 0, 3 and 6. At 24 h post-injection of the third dose, the PC-3 tumors were exposed to an 808 nm laser (0.5 W/cm<sup>2</sup>) for 10 min. After the *in vivo* experiment, the collected tumor tissue was homogenized by PreCellys (Bertin Technologies, Montigny-Le-Bretonneux, France) in 500  $\mu$ L of TRIzol, and then centrifuged at 12,000g at 4 °C for 15 min, and then RNA was extracted from lysates and purified. To synthesize cDNA, 1  $\mu$ g of RNA was used by Verso cDNA synthesis Kit (Thermo Fisher Scientific, Waltham, MA). The sequences of the forward and reverse primers of PLK1 were 5'-CTGCCTGACCATTCCACCAA and 5'-GTGCCGTCACGCTCTATGTA, respectively. The sequences of the forward and reverse primers of  $\beta$ -actin were 5'-ACAGAGCCTCGCCTTTGC and 5'-AGAGGCGTACAGGGATAGCA, respectively. The PCR reaction (94 °C for 30 s, 60 °C for 30 s, 72 °C for 30 s) was run for 30 cycles after an initial single cycle of 94 °C for 2 min to activate the Taq polymerase. For final elongation, single step was performed at 72 °C for 15 min. After amplification, PCR products were analyzed by gel electrophoresis in 1.8% agarose gels and visualized by GelRed™ (Biotium, Hayward, CA) staining.

### Statistical Analysis

The statistical significance of differences between experimental and control groups was determined with Sigma Plot using t-test (p < 0.05 was considered statistically significant).

### Supplementary Material

Supplementary figures.

<http://www.thno.org/v07p4240s1.pdf>

### Acknowledgment

This work was supported in part, by the Intramural Research Program (IRP) of the National Institute of Biomedical Imaging and Bioengineering (NIBIB), National Institutes of Health (NIH) and the Global Innovative Research Center (GiRC) Program (2012K1A1A2A01055811) of the National Research Foundation of Korea.

## Competing Interests

The authors have declared that no competing interest exists.

## References

- Moazed D. Small RNAs in transcriptional gene silencing and genome defence. *Nature*. 2009;457:413-420.
- Kong YW, Ferland-McCollough D, Jackson TJ, Bushell M. microRNAs in cancer management. *Lancet Oncol*. 2012;13:e249-258.
- de Fougerolles A, Vornlocher H-P, Maraganore J, Lieberman J. Interfering with disease: a progress report on siRNA-based therapeutics. *Nat Rev Drug Discov*. 2007;6:443-453.
- Bumcrot D, Manoharan M, Koteliensky V, Sah DW. RNAi therapeutics: a potential new class of pharmaceutical drugs. *Nat Chem Biol*. 2006;2:711-719.
- Takakura Y, Nishikawa M, Yamashita F, Hashida M. Influence of physicochemical properties on pharmacokinetics of non-viral vectors for gene delivery. *J Drug Targeting*. 2002;10:99-104.
- Howard KA, Rahbek UL, Liu X, et al. RNA interference in vitro and in vivo using a chitosan/siRNA nanoparticle system. *Mol Ther*. 2006;14:476-484.
- Semple SC, Akinc A, Chen J, et al. Rational design of cationic lipids for siRNA delivery. *Nat Biotechnol*. 2010;28:172-176.
- Suh MS, Shim G, Lee HY, et al. Anionic amino acid-derived cationic lipid for siRNA delivery. *J Control Release*. 2009;140:268-276.
- Lin Q, Chen J, Zhang Z, Zheng G. Lipid-based nanoparticles in the systemic delivery of siRNA. *Nanomedicine*. 2014;9:105-120.
- Choi YJ, Kang SJ, Kim YJ, Lim Y-b, Chung HW. Comparative studies on the genotoxicity and cytotoxicity of polymeric gene carriers polyethylenimine (PEI) and polyamidoamine (PAMAM) dendrimer in Jurkat T-cells. *Drug Chem Toxicol*. 2010;33:357-366.
- Hunter AC. Molecular hurdles in polyfectin design and mechanistic background to polycation induced cytotoxicity. *Adv Drug Del Rev*. 2006;58:1523-1531.
- Moghim SM, Symonds P, Murray JC, Hunter AC, Debska G, Szewczyk A. A two-stage poly (ethylenimine)-mediated cytotoxicity: implications for gene transfer/therapy. *Mol Ther*. 2005;11:990-995.
- Kuo JhS, Jan Ms, Chiu HW. Mechanism of cell death induced by cationic dendrimers in RAW 264.7 murine macrophage-like cells. *J Pharm Pharmacol*. 2005;57:489-495.
- Juliano R, Alam MR, Dixit V, Kang H. Mechanisms and strategies for effective delivery of antisense and siRNA oligonucleotides. *Nucleic Acids Res*. 2008;36:4158-4171.
- Liu G, Choi KY, Bhirde A, et al. Sticky nanoparticles: a platform for siRNA delivery by a bis(zinc(II) dipicolylamine)-functionalized, self-assembled nanoconjugate. *Angew Chem Int Ed Engl*. 2012;51:445-449.
- Choi KY, Silvestre OF, Huang X, et al. Versatile RNA interference nanoplatform for systemic delivery of RNAs. *ACS Nano*. 2014;8:4559-4570.
- Rhee H-W, Choi SJ, Yoo SH, et al. A bifunctional molecule as an artificial flavin mononucleotide cyclase and a chemosensor for selective fluorescent detection of flavins. *J Am Chem Soc*. 2009;131:10107-10112.
- Kwon TH, Kim HJ, Hong JI. Phosphorescent thymidine triphosphate sensor based on a donor-acceptor ensemble system using intermolecular energy transfer. *Chemistry*. 2008;14:9613-9619.
- Rhee HW, Lee SH, Shin IS, et al. Detection of kinase activity using versatile fluorescence quencher probes. *Angew Chem Int Ed Engl*. 2010;122:5039-5043.
- Hwang L, Ayaz-Guner S, Gregorich ZR, et al. Specific enrichment of phosphoproteins using functionalized multivalent nanoparticles. *J Am Chem Soc*. 2015;137:2432-2435.
- Plaunt AJ, Harmatys KM, Wolter WR, Suckow MA, Smith BD. Library synthesis, screening, and discovery of modified Zinc(II)-bis(dipicolylamine) probe for enhanced molecular imaging of cell death. *Bioconjug Chem*. 2014;25:724-737.
- Yuen KKY, Jolliffe KA. Bis[zinc(II)dipicolylamino]-functionalised peptides as high affinity receptors for pyrophosphate ions in water. *Chem Commun (Camb)*. 2013;49:4824-4826.
- Bahadur K, Thapa B, Bhattarai N. Gold nanoparticle-based gene delivery: promises and challenges. *Nanotechnol Rev*. 2014;3:269-280.
- Webb JA, Bardhan R. Emerging advances in nanomedicine with engineered gold nanostructures. *Nanoscale*. 2014;6:2502-2530.
- Huang P, Lin J, Li W, et al. Biodegradable gold nanovesicles with an ultrastrong plasmonic coupling effect for photoacoustic imaging and photothermal therapy. *Angew Chem Int Ed Engl*. 2013;52:13958-13964.
- Song J, Yang X, Jacobson O, et al. Sequential drug release and enhanced photothermal and photoacoustic effect of hybrid reduced graphene oxide-loaded ultrasmall gold nanorod vesicles for cancer therapy. *ACS Nano*. 2015;9:9199-9209.
- Huang P, Lin J, Wang S, et al. Photosensitizer-conjugated silica-coated gold nanoclusters for fluorescence imaging-guided photodynamic therapy. *Biomaterials*. 2013;34:4643-4654.
- Wang S, Huang P, Nie L, et al. Single continuous wave laser induced photodynamic/plasmonic photothermal therapy using photosensitizer-functionalized gold nanostars. *Adv Mater*. 2013;25:3055-3061.
- Liang C, Diao S, Wang C, et al. Tumor metastasis inhibition by imaging-guided photothermal therapy with single-walled carbon nanotubes. *Adv Mater*. 2014;26:5646-5652.
- Li X, Takashima M, Yuba E, Harada A, Kono K. PEGylated PAMAM dendrimer-doxorubicin conjugate-hybridized gold nanorod for combined photothermal-chemotherapy. *Biomaterials*. 2014;35:6576-6584.
- Yang H-W, Liu H-L, Li M-L, et al. Magnetic gold-nanorod/PNIPAAmMA nanoparticles for dual magnetic resonance and photoacoustic imaging and targeted photothermal therapy. *Biomaterials*. 2013;34:5651-5660.
- Zhang Z, Wang J, Chen C. Gold nanorods based platforms for light-mediated theranostics. *Theranostics*. 2013;3:223-238.
- Jia J, Zhu F, Ma X, Cao ZW, Li YX, Chen YZ. Mechanisms of drug combinations: interaction and network perspectives. *Nat Rev Drug Discov*. 2009;8:111-128.
- Al-Lazikani B, Banerji U, Workman P. Combinatorial drug therapy for cancer in the post-genomic era. *Nat Biotechnol*. 2012;30:679-692.
- Woodcock J, Griffin JP, Behrman RE. Development of novel combination therapies. *New Engl J Med*. 2011;364:985-987.
- Batist G, Gelmon KA, Chi KN, et al. Safety, pharmacokinetics, and efficacy of CPX-1 liposome injection in patients with advanced solid tumors. *Clin Cancer Res*. 2009;15:692-700.
- Barr FA, Siljé HH, Nigg EA. Polo-like kinases and the orchestration of cell division. *Nat Rev Mol Cell Biol*. 2004;5:429-441.
- Kasahara K, Goto H, Izawa I, et al. PI 3-kinase-dependent phosphorylation of Plk1-Ser99 promotes association with 14-3-3 $\gamma$  and is required for metaphase-anaphase transition. *Nat Commun*. 2013;4:1882.
- Petronczki M, Lénárt P, Peters J-M. Polo on the rise—from mitotic entry to cytokinesis with Plk1. *Dev Cell*. 2008;14:646-659.
- Martin BT, Strebhardt K. Polo-like kinase 1: target and regulator of transcriptional control. *Cell Cycle*. 2006;5:2881-2885.
- Strebhardt K, Ullrich A. Targeting polo-like kinase 1 for cancer therapy. *Nature reviews cancer*. 2006;6:321-330.
- Eckerdt F, Yuan J, Strebhardt K. Polo-like kinases and oncogenesis. *Oncogene*. 2005;24:267-276.
- Simizu S, Osada H. Mutations in the Plk gene lead to instability of Plk protein in human tumour cell lines. *Nat Cell Biol*. 2000;2:852-854.
- Knecht R, Elez R, Oechler M, Solbach C, von Ilberg C, Strebhardt K. Prognostic significance of polo-like kinase (PLK) expression in squamous cell carcinomas of the head and neck. *Cancer Res*. 1999;59:2794-2797.
- Dietzmann K, Kirches E, Von Bossanyi P, Jachau K, Mawrin C. Increased human polo-like kinase-1 expression in gliomas. *J Neurooncol*. 2001;53:1-11.
- Peters U, Cherian J, Kim JH, Kwok BH, Kapoor TM. Probing cell-division phenotype space and Polo-like kinase function using small molecules. *Nat Chem Biol*. 2006;2:618-626.
- Ellis PM, Chu QS, Leigh N, et al. A phase I open-label dose-escalation study of intravenous BI 2536 together with pemetrexed in previously treated patients with non-small-cell lung cancer. *Clin Lung Cancer*. 2013;14:19-27.
- Frost A, Mross K, Steinbild S, et al. Phase I study of the Plk1 inhibitor BI 2536 administered intravenously on three consecutive days in advanced solid tumours. *Current Oncol*. 2012;19:28-35.
- Olmos D, Barker D, Sharma R, et al. Phase I study of GSK461364, a specific and competitive Polo-like kinase 1 inhibitor, in patients with advanced solid malignancies. *Clin Cancer Res*. 2011;17:3420-3430.
- Ma WW, Messersmith WA, Dy GK, et al. Phase I study of Rigosertib, an inhibitor of the phosphatidylinositol 3-kinase and Polo-like kinase 1 pathways, combined with gemcitabine in patients with solid tumors and pancreatic cancer. *Clin Cancer Res*. 2012;18:2048-2055.
- Song J, Pu L, Zhou J, Duan B, Duan H. Biodegradable theranostic plasmonic vesicles of amphiphilic gold nanorods. *ACS Nano*. 2013;7:9947-9960.
- Ding Y, Jiang Z, Saha K, et al. Gold nanoparticles for nucleic acid delivery. *Mol Ther*. 2014;22:1075-1083.
- Whitehead KA, Langer R, Anderson DG. Knocking down barriers: advances in siRNA delivery. *Nat Rev Drug Discov*. 2009;8:129-138.